

Deep Grasp: Detection and Localization of Grasps with Deep Neural Networks

Fu-Jen Chu[†] and Patricio A. Vela[†]

Abstract—A deep learning architecture is proposed to predict graspable locations for robotic manipulation. We consider a more realistic situation that none or multiple objects can be in a scene. By transforming grasp configuration regression into classification problem with null hypothesis competition, the deep neural network with RGB-D image input predicts multiple grasp candidates on a single unseen object, as well as predict grasp candidates on multiple novel objects in a single shot. We perform extensive experiments with our framework on different scenarios, including no object, single object, and multi-objects. We compare with state-of-the-art approaches on Cornell dataset, and show we can achieve 96.0% and 96.1% accuracy on image-wise split and object-wise split, respectively.

I. INTRODUCTION

While manipulating objects is relatively easy for humans, reliably grasping arbitrary objects remains an open challenge for robots. Resolving it would advance the application of robotics to industry use cases, such as industrial part assembly, binning, and sorting. Likewise, it would advance the area of assistive robotics, where the robot interacts with its surroundings in support of human needs. Robotic grasping involves perception, planning, and control. As a starting point, knowing which object to grab and how to do so is essential. Consequently, accurate and diverse detection of robotic grasp candidates for target objects should lead to a better path design, benefit gripper control, and improve the overall performance of manipulation task.

The proposed grasping solution utilizes a deep learning strategy for identifying suitable grasp configurations from an input image. Over the past decade, deep learning has achieved major success on detection, classification, and regression tasks [1]–[3]. Its key strength is the capability to leverage large quantities of labelled and unlabelled data to learn powerful representations without hand-engineering the feature space. Deep neural networks have been shown to outperform hand-designing features and reach state-of-the-art performance. It is also shown suitable for incorporating common robotics imaging modalities such as RGB and depth sensor data.

In this research problem, we are interested in tackling the challenging problem of searching for robotic grasps of objects in an RGB-D image. Given an object, we are interested in inferring viable robotic grasps for it. The envisioned gripper would be a parallel (or similar in functionality) gripper. Identifying grasp candidates is challenging since the



Fig. 1. Detection of multiple grasps for multiple objects simultaneously using the proposed model. The model was trained on Cornell dataset [4] in standard object-wise split, then applied to this novel image.

varying shapes and poses of novel objects. Furthermore, the features of grasps on each object could be different, causing the detection task even difficult. The proposed architecture associated to the grasp configuration estimation problem relies on the strengths of deep convolutional neural networks (CNNs) at detection and classification. Within this architecture, the identification of grasp configuration for objects is broken down into a grasp detection processes followed by a more refined grasp orientation classification process, both embedded within two coupled networks.

The proposed architecture includes a grasp region proposal network for identification of potential grasp regions. The network then partitions the grasp configuration estimation problem into regressing on the bounding box parameters, and classifying for the orientation angles, from RGB-D data. Importantly, the orientation classifier also includes a “No Orientation” class which rejects spuriously identified regions for which no single orientation classification performs well, and acts as a competing non-grasp collector class. The proposed approach predicts grasp candidates in more realistic situations. The situations consider that no, single, and multiple objects may be visible; and the system predicts multiple grasps with confidence scores accordingly (see Fig. 1). A new multi-objects grasp dataset is collected for evaluation with the traditional performance metric of false-positives-per-image. We conjecture that the multi-grasp output and associated confidence scores could inform a subsequent planning process that could take advantage of the rich multi-grasp output for improved manipulator planning and grasping success.

The main contributions of this paper is threefold:

* This work supported in part by NSF Award #1605228.

† Institute for Robotics and Intelligent Machines, Georgia Institute of Technology, GA, USA. {fujenchu, pvela}@gatech.edu

(1) A novel deep architecture is proposed to predict grasp candidates in a more realistic situation. It considers none, single and multiple objects in the view, and predict multiple grasps with confidence scores for real world robotic manipulation.

(2) A multi-object, multi-grasp dataset is collected for grasp detection. This smaller dataset contains RGB-D images with multiple objects in a scene. Each object is manually annotated with grasp configuration ground-truth in the same way as Cornell Dataset. The dataset will be released in public for multi-object multi-grasp detection benchmark.

(3) The proposed approach is evaluated using the Cornell dataset and shown to provide state-of-the-art performance for both image-wise and object-wise tests. Furthermore, experiments are performed on new collected multi-object dataset to demonstrate the generalization and multi-object, multi-grasp capabilities of the proposed architecture.

II. RELATED WORK

Research on grasping has evolved significantly over the last two decades. Altogether, the review papers [5]–[8] provide a good context for the overall field. Rather than providing a deep and comprehensive history, this section reviews grasping with an emphasis on learning-based approaches and on representation learning.

Early work on perception-based learning approaches to grasping goes back to [9], which identified a low dimensional feature space for identifying and ranking grasps. Importantly it showed that learning-based methods could generalize to novel objects. Since then, machine learning methods have evolved alongside grasping strategies. Exploiting the input/output learning properties of machine learning (ML) systems, [10] proposed to learn the image to grasp mapping through the manual design of a convolutional network. As an end-to-end system, reconstruction of the object’s 3D geometry is not needed to arrive at a grasp hypothesis. The system was trained using synthetic imagery, then demonstrated successful grasping on real objects. Likewise, [11] employed a CNN-like feature space with random forests for grasp identification. As important as where to grasp is how to grasp. Several efforts move to learn the grasp approach or pre-grasp strategy [12], [13], while some focus on whether the hypothesized grasp is likely to succeed [14]. Many of these approaches exploited contemporary machine learning algorithms with manually defined feature spaces.

At the turn of this decade, two advances led to new methods for improving grasp identification: the introduction of low-cost depth cameras, and the advent of computational frameworks to facilitate the construction and training of convolutional neural networks (CNNs). The advent of consumer depth cameras enabled the encoding of richer grasp output models in the “image” to grasp mapping. In particular [15] represented grasps as a 2D oriented rectangle in image space with the local surface normal as the approaching vector; this grasp configuration vector has been adopted as the well-accepted formulation. Generally, the early methods using depth cameras sought to recover the 3D geometry from point

clouds for grasp planning [16], with manually derived feature space used in the learning process. Deep learning approaches arrived later [2] and have been quickly adopted in many fields by the computer vision community [17].

Deep learning avoids the need for engineering feature spaces, with the trade-off that larger datasets are needed. The trade-off is usually mitigated through the use of pre-training on pre-existing computer vision datasets followed by fine-tuning on a smaller, problem-specific dataset. Following a sliding window approach, [18] trained a two stage multi-modal network, with the first stage generating hypothesis to further process by a more accurate second stage. Similarly, [19] first performed a image-wide pre-processing step to identify candidate object regions, followed by application of a CNN per region. To avoid sliding windows or image-wide search, end-to-end approaches are trained to output a single grasp configuration from the input data [20], [21]. To do so, [20] used a regression based strategy which needs to be compensated through image partitioning as the grasp configuration space is non-convex. The two-stage network in [21] first output a learnt feature, which is then used to provide a single grasp output. These may suffer from averaging effects associated to the single-output nature of the mapping. Guo et al. [22] employed a two-stage process with a feature learning CNN, followed by specific deep network outputs (graspable, bounding box, and orientation). Most deep network approaches mentioned above start with the strong prior that every image contains a single object with a single grasp target (except [19]). This assumption may not hold in practice that many objects have multiple grasp locations, and the image may contain more than one object.

An alternative to grasp parameter output networks are grasp quality networks [23], [24]. Given a region of interest, they provide a grasp quality score over the set of all possible grasps (which may be discretized). Such networks admit the inclusion of end-effector uncertainty.

Inspired by [25], we proposed to incorporate a *grasp region proposal network* to generate candidate regions for feature extraction, instead of mapping scores value to each local pixel. Furthermore, we propose to transform grasp configuration regression problem formulated in previous works [20], [21] into a combination of region detection and orientation classification problems. We utilize ResNet [17], the current state-of-the-art deep convolutional neural network, for feature extraction and grasp prediction. Compared to previous approaches, our method considers more realistic scenarios with multiple objects in a scene. And the proposed architecture predicts multiple grasps with corresponding confidence scores, which benefits subsequent planning process for robotic application.

III. PROBLEM STATEMENT

Given corresponding RGB and depth images of a novel object, the objective is to identify the grasp configuration for potential grasp candidates of an object for the purpose of manipulation. The 5-dimensional *grasp rectangle* [15] is the grasp configuration representation employed. It is a

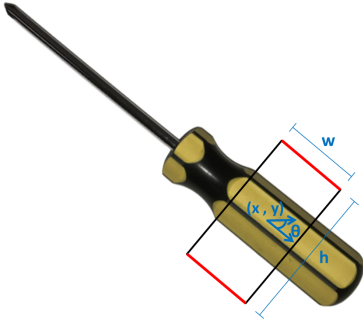


Fig. 2. The 5D grasp representation. The red lines correspond to parallel plates of the gripper. The black lines show the distance between the plates of the gripper before the grasp is executed.

simplification of the 7-dimensional representation [15] and describes the location, orientation, and opening distance of a parallel plate gripper prior to closing on an object. The 2D orientated rectangle, shown in Fig. 2 depicts the gripper's location (x, y) , orientation θ , and opening distance h . An additional parameter describing the remaining length w completes the bounding box grasp configuration,

$$g = \{x, y, \theta, w, h\}^T. \quad (1)$$

Thinking of the center of the bounding box with its local (x, y) axes aligned to the w and h variables, respectively the first three parameters represent the $SE(2)$ frame of the bounding box in the image, while the last two describe the dimensions of the box.

IV. APPROACH

Much like [20], [22], the proposed approach should avoid sliding window such as in [18] for real-time implementation purposes. We avoid the time-consuming sliding-window approach by harnessing the capacity of neural networks at the task of bounding box regression, and thereby predict potential candidates on the full image directly. Furthermore, we preserve all possible grasps and output all ranked candidates, instead of the averaged regression result. To induce a richer feature representation and learn more of the structural cues, we propose to use a deeper network model compared to previous works [18], [20], [26], with the aim of improving feature extraction for robotic grasp detection. We adopt the ResNet-50 [17] with fifty layers, which has more capacity and is potentially able to learn better than the AlexNet [2] used in previous works (eight layers). ResNet is known for its residual learning concept to overcome the challenge of learning mapping functions. A residual block is designed as an incorporation of a skip connection with standard convolutional neural network. This design allows the block to bypass the input, and encourage convolutional layers to predict the residual for the final mapping function of a residual block.

The next three subsections describe the overall architecture of the system. Subsections includes integration of proposal network to generate candidate regions for grasps. Then we

discuss our choice to define grasp parameter estimation as a combination of regression and classification problems. Lastly, we explain the multi-grasp detection architecture.

A. Grasp Proposals

The first stage of the deep network aims to generate grasp proposals across the whole image, avoiding the need for a separate object segmentation pipeline. Inspired by *Region Proposal Network* (RPN) [25], we reset each orientated ground truth bounding box to have vertical height and horizontal width, as shown in Fig. 4. RPN shares a common set of convolutional layers of ResNet-50 in our architecture, and outputs a 512-d feature which is then fed into two sibling fully connected layers. The two outputs specify both probability of grasp proposal and proposal bounding box for each anchor.

At each anchor, by default 3 scales and 3 aspect ratios are used for grasp reset bounding box shape variations. RPN works as sliding a mini-network over the final convolutional feature map of ResNet-50. Hence $W \times H \times 9$ predictions would be generated in total. Let t_i denote the 4-dimensional vector specifying the reset (x, y, w, h) of the i -th grasp configuration, and g_i denote the probability of the i -th grasp proposal, we define the loss of grasp proposal net to be:

$$L_{gpn}(\{(g_i, t_i)\}_{i=1}^I) = \sum_i L_{gp_cls}(g_i, g_i^*) + \lambda \sum_i g_i^* L_{gp_reg}(t_i, t_i^*). \quad (2)$$

where $g_i^* = 0$ if no grasp and $g_i^* = 1$ if grasp is specified. t_i^* is the ground truth grasp coordinates corresponding to g_i^* .

B. Grasp Orientation as Classification

Many prior approaches [20], [21] regress to a single 5-dimensional grasp representation $g = \{x, y, w, h, \theta\}$ for an input RGB-D image. Yet to predict either on $SE(2)$ (planar pose) or on S^1 (orientation) involves predicting coordinates that lie in a non-Euclidean (non-convex) space where regression and its standard L2 loss may not perform well. Thus, rather than perform regression, in our pipeline for multi-grasp, we propose to quantize the orientations θ of grasp representation into R angles, and formulate the input/output mapping a classification task for grasp orientation. This is similar to [22], except that we also add a non-grasp collecting orientation class. If none of the orientation classifiers outputs a score higher than the non-grasp class, then the grasp proposal is considered incorrect and rejected. The value of the non-grasp class is that it is also necessary for the downstream multi-object, multi-grasp component of the final algorithm. The total number of classes is $|\mathcal{C}| = R + 1$. Denote by $\{(l_i, \theta_i)\}_{i=1}^I$ where the i -th grasp configuration with classification label $l_i \in 1, \dots, R$ is associated with the angle θ_i . For the case of no possible orientation (i.e., the region is not graspable), the output label is $l = 0$ and there is no associated orientation. Here, $R = 19$ as illustrated in Fig.

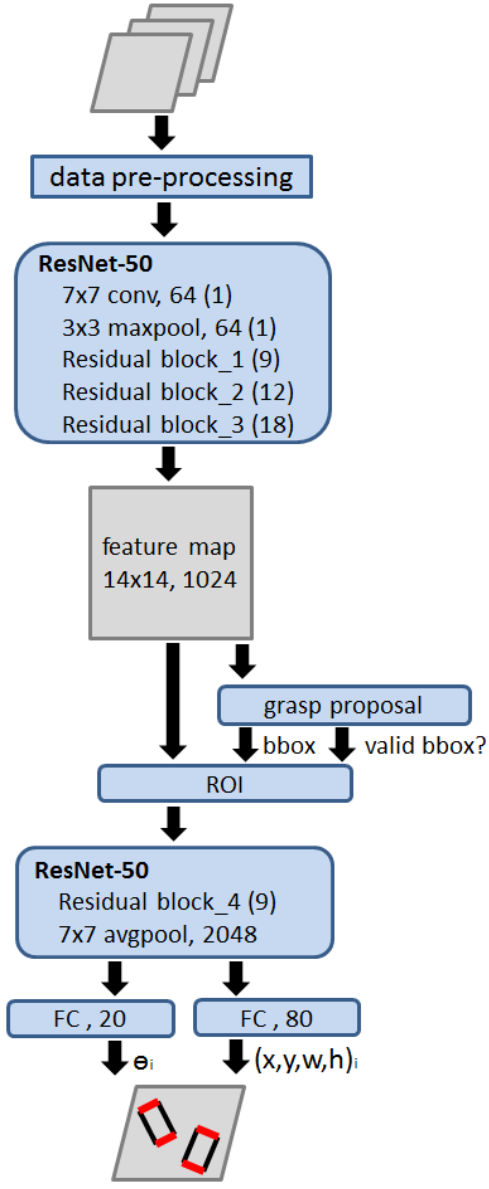


Fig. 3. Complete structure of our multi-object multi-grasp predictor.

5, yet it could be a larger number to yield better performance potentially.

C. Multi-Grasp Detection

After the region proposal stage of the deep network, the last stage aims to identify grasp configurations for candidates. This last stage classifies the predicted region proposals from previous stage INTO R regions for grasp configuration parameter θ . At the same time the last stage also refines the proposal bounding box to a non-oriented grasp bounding box (x, y, w, h) .

To process the region proposals efficiently, we integrate the *ROI pooling layer* [27] into ResNet-50 model so that it may share ResNet's convolutional layers. Sharing the feature map with previous layers avoids re-computation of features within the region of interest. An *ROI pooling layer* stacks all of

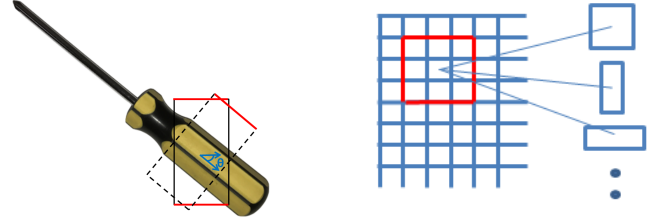


Fig. 4. Left: a grasp rectangle is first set to its reset position for grasp proposal training. The angle θ falls into one of the rotation angle categories. Right: each element in feature map works as anchor and corresponds to multiple candidate grasp proposal bounding boxes.

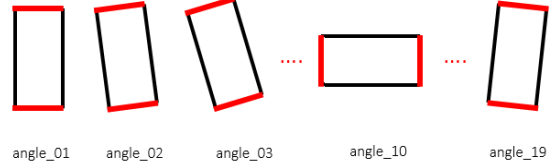


Fig. 5. Instead of regressing the angle of rectangle representation into a scalar, we transform regression problem into classification problem. Orientated grasps are classified into 19 classes depending on the rotated angles. The figure illustrates the angle for each class.

the features of the identified grasp proposals, which then get fed to two sibling fully connected layers for orientation parameter classification l and bounding box regression (x, y, w, h) . The ROI pooling layer receives its input from the last convolutional layer of ResNet-50 (layer 41).

Let p_l denote the probability of class l after softmax layer, and t_l denote the corresponding predicted grasp bounding box. Define the loss function of the grasp configuration prediction to be:

$$L_{gcr}(\{(p_l, t_l)\}_{c=0}^C) = \sum_c L_{gcr_cls}(p_l) + \lambda_2 \sum_c \mathbf{1}_{c \neq 0}(c) L_{gcr_reg}(t_c, t_c^*). \quad (3)$$

where t_c^* is the ground truth grasp bounding box.

With the modified architecture of ResNet-50 model, end-to-end training for grasp detection and grasp parameter estimation employs the total loss:

$$L_{total} = L_{gpn} + L_{gcr} \quad (4)$$

The streamlined system generates grasp proposals at the ROI layer, stacks all ROIs using the shared feature, and the additional neurons of the two sibling layers output grasp bounding boxes and orientations, or reject the proposed region.

V. EXPERIMENTS AND EVALUATION

Evaluation of the grasp identification algorithm utilizes the Cornell Dataset for benchmarking against other state-of-the-art algorithms. To demonstrate the multi-object, multi-grasp capabilities, a new dataset is carefully collected and manually annotated. Both datasets consist of color and depth

images for multiple modalities. In practical not all possible grasps are covered by the labelled ground truth, yet the grasp rectangles are comprehensive and representative for diverse examples of good candidates. The scoring criteria takes into account the potential sparsity of the grasp configuration by including an acceptable proximity radius to the ground truth grasp configuration.

a) Cornell Dataset: The Cornell Dataset [4] consists of 885 images of 244 different objects, with several images taken of each object in various orientations or poses. Each distinct image is labelled multiple ground truth grasps corresponding to possible ways to grab the object. A ground truth is represented by an oriented rectangle in the image plane which defines the orientation of a gripper parallel to the image plane.

b) Multi-Object Dataset: Since the Cornell Dataset scenarios consist of one object in one image, we collect a Multi-Object Dataset for the evaluation of the multi-object/multi-grasp case. Our dataset is meant for evaluation and consists of 96 images with 3-5 different objects in a single image. We follow the same protocol as the Cornell Dataset by taking several images of each set of objects in various orientations or poses. Multiple ground truth grasps for each object in each image are annotated using the same configuration definition.

A. Cornell Data Preprocessing

To reuse the pre-trained weights of ResNet-50 on COCO-2014 dataset [28], Cornell dataset is preprocessed to fit the input format of the ResNet-50 network. For fair comparison, we followed the same procedure in [20] and the blue channel is substituted with depth channel of the original image. Ideally red or green channels can be selected. Since RGB data lies between 0 to 255, the depth information is normalized to the same range. The mean image is chosen to be 144, while the pixels on the depth image with no information were padded with zeros. For the data preparation, we perform extensive data augmentation. First, the images are center cropped to obtain a 351x351 region. Then the cropped image is randomly rotated between 0 to 360 degree and center cropped to 321x321 in size. The rotated image is randomly translated in x and y direction by up to 50 pixels. Finally the image is resized to 227x227 to fit the input of ResNet-50 architecture.

B. Pre-Training

To avoid over-fitting and achieve better minimum point, we start with the pretrained ResNet-50. As shown in Fig 3, we implement grasp proposal layer after the third residual block by sharing the feature map. The proposals are then sent to ROI layer and fed into the fourth residual layer. The 7×7 average pool output are then fed to two fully connected layers for final classification and regression. All new layers beyond ResNet-50 are trained from scratch.

Because the orientation is specified as a class label and assigned a specific orientation, the Cornell dataset needs to be converted into the expected output format of the proposed

network. We equally divide 180 degrees into R regions (due to symmetry of the parallel gripper) and assign the continuous ground truth orientation to the nearest discrete orientation.

C. Training

For training, we train the whole network end-to-end for 5 epochs on a single nVidia Titan-X (Maxwell architecture). The initial learning rate is set to 0.0001. And we divide the learning rate by 10 every 10000 iterations. We use Tensorflow as our implementation framework with cudnn-5.1.10 and cuda-8.0 packages. All the code and multi-object dataset will be publicly released.

D. Evaluation Metric

Accuracy evaluation of the grasp parameters involves checking for proximity to the ground truth according to established criteria [20]. A hypothesized grasp configuration is reported correct if both:

- 1) the difference of angle between predicted grasp G_p and ground truth G_t is within 30° , and
- 2) the Jaccard index of the predicted grasp G_p and the ground truth G_t is greater than 0.25, e.g.,

$$J(G_p, G_t) = \frac{|G_p \cap G_t|}{|G_p \cup G_t|} > 0.25 \quad (5)$$

The Jaccard index is similar to the Intersection over Union (IoU) threshold for object detection.

VI. RESULTS

A. Single-object Single-grasp

We tested proposed architecture on the Cornell Dataset, and the comparison results with prior works leads to Table I. For this comparison, which is a single-object/single-grasp test, the highest output score of all grasp candidates output is chosen as the final output. The proposed architecture outperforms all competitive methods. On image-wise split, our architecture reaches 96.0% accuracy; on object-wise split for unseen objects, 96.1% accuracy is achieved. We also tested our proposed architecture by replacing ResNet-50 with VGG-16 architecture, a smaller deep net with 16 layers. With VGG-16, our model still outperforms competitive approaches. Yet the deeper ResNet-50 achieve 4.4% more on unseen objects. The third row contains the run-time of methods that have reported it, as well as the runtime of the proposed method. Computationally, our architecture detect and localize multiple grasps in 0.120s, which is around 8 fps and is close to usable in real time applications. Table II contains the outcomes of stricter Jaccard indexes for the ResNet-50 model. Performance decreases with stricter conditions but maintains competitiveness even at 0.40 IoU condition.

Typical output of the system is given in Fig. 6a, where four grasps are identified. Limiting the output to a single grasp leads to the outputs depicted in Fig. 6b. In the multi-grasp case, our system not only predicts universal grasps learned from ground truth, but also contains candidate grasps not contained in the ground truth, Fig. 6c.

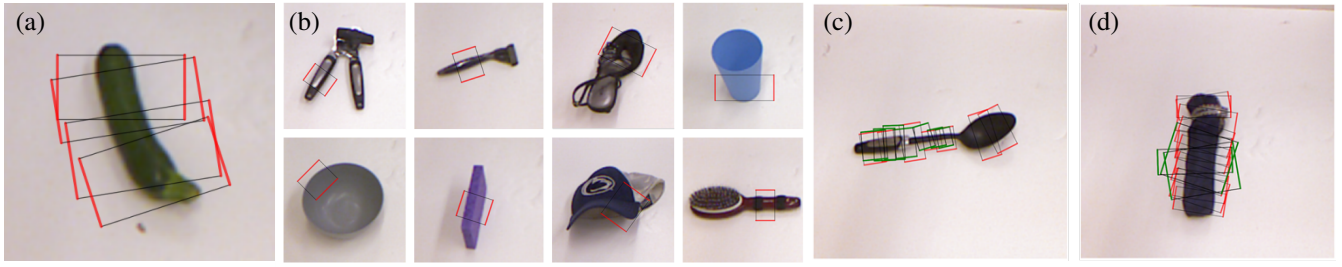


Fig. 6. Sample 5D grasp configuration outputs of system for Cornell dataset inputs: (a) the multiple grasp options output for an object; (b) the top grasp outputs for several objects; (c) and (d) example output grasps (red) and ground-truth grasps (green) demonstrate that the system may output grasps for which there is no ground truth.

TABLE I
SINGLE-OBJECT SINGLE-GRASP EVALUATION

approach	image-wise	object-wise	speed
Prediction Accuracy (%)			fps
Jiang et al. [15]	60.5	58.3	0.02
Lenz et al. [18]	73.9	75.6	–
Redmon et al. [20]	88.0	87.1	3.31
Wang et al. [19]	81.8	N/A	7.10
Asif et al. [11]	88.2	87.5	–
Kumra et al. [21]	89.2	88.9	16.03
Mahler et al. [24]	93.0	N/A	~0.4
Guo et al. [22]	93.2	89.1	–
Ours: VGG-16	95.5	91.7	17.24
Ours: ResNet-50	96.0	96.1	8.33

TABLE II
PREDICTION ACCURACY (%) AT DIFFERENT JACCARD THRESHOLDS

split	0.25	0.30	0.35	0.40
image-wise	96.0	94.9	92.1	84.7
object-wise	96.1	92.7	87.6	82.6

B. Single-object multi-grasp

For realistic robotic application, a viable grasp usually depends both on the object and its surroundings. Given that one grasp candidate may be impossible to achieve, there is benefit to provide a rank ordered list of grasp candidates. Our system provides a list of high quality grasp candidates for a subsequent planner to select from. Fig. 7c shows samples of the predicted grasps and corresponding ground truths. To evaluate the performance of the multi-grasp detector, we employ the same scoring system as with the single grasp, then generate the miss rate as a function of the number of false positives per image (FPPI) by varying the detection threshold, see Fig. 7a for the single-object multi-grasp case. The model achieves 28% and 25% miss rate at 1 FPPI for object-wise split and image-wise split, respectively. The model performs slightly better in image-wise split than object-wise split due to unseen objects in the latter.

C. Multi-object multi-grasp

Lastly, we apply the proposed architecture to a multi-object multi-grasp task using our Multi-Object dataset. The trained network is the same trained network we've been reporting the results for (trained only on the Cornell dataset

with both image-split and object-split variants). Testing involves evaluating against the multi-object dataset, and represents a cross domain application with unseen objects.

Fig. 7b depicts the plot of miss rate versus FPPI. At 1FPPI, the system achieves 53% and 49% prediction accuracy with image-split model and object-split networks, respectively. Note that the ground truth annotation on the multi-object dataset are not extensive and the environment settings are different. Visualizations of predicted grasp candidates are depicted in Fig. 8. The model successfully locates multiple grasp candidates on multiple new objects in the scene with very few false positives, and hence is practical for robotic manipulations.

VII. CONCLUSION

We present a novel grasping detection system to predict grasp candidates for novel objects in RGB-D images. Compared to previous works, our architecture is able to predict multiple potential grasps instead of single averaged regression, which could benefit subsequent planning process in practical usage. Our regression as classification approach transforms angle regression problem to a classification task, which can take advantage of the natural of CNNs for better performance. We evaluate our system on Cornell Grasping Dataset with state-of-the-arts to prove the effectiveness of our design. We also perform experiments on self-collected multi-object dataset for multi-object multi-grasp scenario. All code and dataset will be publicly released.

REFERENCES

- [1] L. Bo, X. Ren, and D. Fox, “Unsupervised feature learning for rgbd based object recognition,” in *Experimental Robotics*. Springer, 2013, pp. 387–402.
- [2] A. Krizhevsky, I. Sutskever, and G. E. Hinton, “Imagenet classification with deep convolutional neural networks,” in *Advances in neural information processing systems*, 2012, pp. 1097–1105.
- [3] J. Ngiam, A. Khosla, M. Kim, J. Nam, H. Lee, and A. Y. Ng, “Multimodal deep learning,” in *Proceedings of the 28th international conference on machine learning (ICML-11)*, 2011, pp. 689–696.
- [4] R. L. Lab, “Cornell grasping dataset,” http://pr.cs.cornell.edu/grasping/rect_data/data.php, 2013, accessed: 2017-09-01.
- [5] K. B. Shimoga, “Robot grasp synthesis algorithms: A survey,” *The International Journal of Robotics Research*, vol. 15, no. 3, pp. 230–266, 1996.
- [6] A. Bicchi and V. Kumar, “Robotic grasping and contact: A review,” in *ICRA*. Citeseer, 2000, pp. 348–353.
- [7] A. Sahbani, S. El-Khoury, and P. Baidaud, “An overview of 3d object grasp synthesis algorithms,” *Robotics and Autonomous Systems*, vol. 60, no. 3, pp. 326–336, 2012.

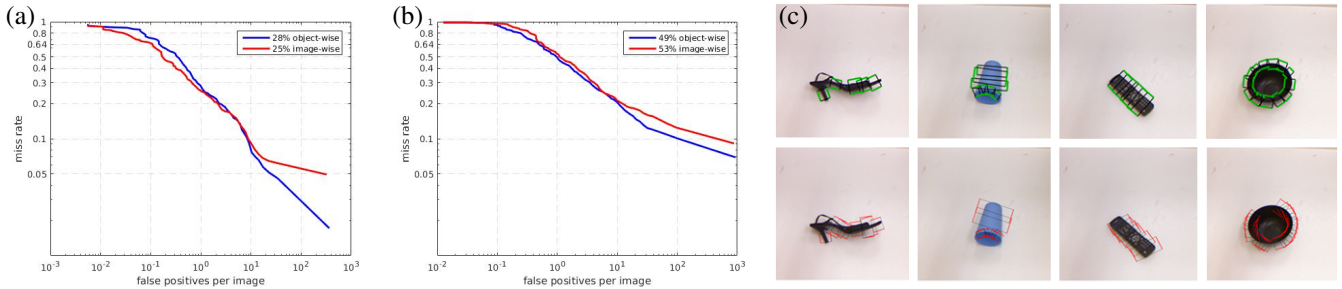


Fig. 7. Detection results of the system. Green rectangles are ground truths and red rectangles are predicted grasps. Detection results of our system on multi-object multi-grasp scenario. The model was trained on Cornell Dataset and tested on our own multi-object dataset. Red rectangle represent the predicted grasp on each unseen object.



Fig. 8. Detection results of our system on multi-object multi-grasp scenario. The model was trained on Cornell Dataset and tested on our own multi-object dataset. Red rectangle represent the predicted grasp on each unseen object.

- [8] J. Bohg, A. Morales, T. Asfour, and D. Kragic, "Data-driven grasp synthesis-a survey," *IEEE Transactions on Robotics*, vol. 30, no. 2, pp. 289–309, 2014.
- [9] I. Kamon, T. Flash, and S. Edelman, "Learning to grasp using visual information," in *Robotics and Automation, 1996. Proceedings., 1996 IEEE International Conference on*, vol. 3. IEEE, 1996, pp. 2470–2476.
- [10] A. Saxena, J. Driemeyer, and A. Y. Ng, "Robotic grasping of novel objects using vision," *The International Journal of Robotics Research*, vol. 27, no. 2, pp. 157–173, 2008.
- [11] U. Asif, M. Bennamoun, and F. A. Sohel, "Rgb-d object recognition and grasp detection using hierarchical cascaded forests," *IEEE Transactions on Robotics*, 2017.
- [12] S. Ekvall and D. Kragic, "Learning and evaluation of the approach vector for automatic grasp generation and planning," in *Proceedings 2007 IEEE International Conference on Robotics and Automation*. IEEE, 2007, pp. 4715–4720.
- [13] K. Huebner and D. Kragic, "Selection of robot pre-grasps using box-based shape approximation," in *2008 IEEE/RSJ International Conference on Intelligent Robots and Systems*. IEEE, 2008, pp. 1765–1770.
- [14] Q. V. Le, D. Kamm, A. F. Kara, and A. Y. Ng, "Learning to grasp objects with multiple contact points," in *Robotics and Automation (ICRA), 2010 IEEE International Conference on*. IEEE, 2010, pp. 5062–5069.
- [15] Y. Jiang, S. Mosenon, and A. Saxena, "Efficient grasping from RGBD images: Learning using a new rectangle representation," in *Proceedings of IEEE International Conference on Robotics and Automation*, 2011, pp. 3304–3311.
- [16] D. Rao, Q. V. Le, T. Phoka, M. Quigley, A. Sudsang, and A. Y. Ng, "Grasping novel objects with depth segmentation," in *Intelligent Robots and Systems (IROS), 2010 IEEE/RSJ International Conference on*. IEEE, 2010, pp. 2578–2585.
- [17] K. He, X. Zhang, S. Ren, and J. Sun, "Deep residual learning for image recognition," in *Proceedings of the IEEE conference on computer vision and pattern recognition*, 2016, pp. 770–778.
- [18] I. Lenz, H. Lee, and A. Saxena, "Deep learning for detecting robotic grasps," *International Journal of Robotics Research*, vol. 34, no. 4-5, pp. 705–724, 2015.
- [19] Z. Wang, Z. Li, B. Wang, and H. Liu, "Robot grasp detection using multimodal deep convolutional neural networks," *Advances in Mechanical Engineering*, vol. 8, no. 9, p. 1687814016668077, 2016.
- [20] J. Redmon and A. Angelova, "Real-time grasp detection using convolutional neural networks," in *2015 IEEE International Conference on Robotics and Automation (ICRA)*. IEEE, 2015, pp. 1316–1322.
- [21] S. Kumra and C. Kanan, "Robotic grasp detection using deep convolutional neural networks," in *Proceedings of the IEEE International Conference on Intelligent Robotic and Systems*, 2017.
- [22] D. Guo, F. Sun, H. Liu, T. Kong, B. Fang, and N. Xi, "A hybrid deep architecture for robotic grasp detection," in *Proceedings of IEEE International Conference on Robotics and Automation*, 2017, pp. 1609–1614.
- [23] E. Johns, S. Leutenegger, and A. J. Davison, "Deep learning a grasp function for grasping under gripper pose uncertainty," in *Proceedings of the IEEE International Conference on Intelligent Robotic and Systems*, 2016, pp. 4461–4468.
- [24] J. Mahler, J. Liang, S. Niyaz, M. Laskey, R. Doan, X. Liu, J. Aparicio-Ojea, and K. Goldberg, "Dex-Net 2.0: Deep learning to plan robust grasps with synthetic point clouds and analytic grasp metrics," in *Robotics: Science and Systems*, 2017.
- [25] S. Ren, K. He, R. Girshick, and J. Sun, "Faster R-CNN: Towards real-time object detection with region proposal networks," in *Advances in Neural Information Processing Systems*, 2015, pp. 91–99.
- [26] L. Pinto and A. Gupta, "Supersizing self-supervision: Learning to grasp from 50k tries and 700 robot hours," in *Robotics and Automation (ICRA), 2016 IEEE International Conference on*. IEEE, 2016, pp. 3406–3413.
- [27] R. Girshick, "Fast R-CNN," in *IEEE International Conference on Computer Vision*, 2015, pp. 1440–1448.
- [28] T.-Y. Lin, M. Maire, S. Belongie, J. Hays, P. Perona, D. Ramanan, P. Dollár, and C. L. Zitnick, "Microsoft coco: Common objects in

context,” in *European conference on computer vision*. Springer, 2014, pp. 740–755.